

1 **Delta Blue Intensity vs. Maximum Density: A Case Study using *Pinus uncinata* in the Pyrenees**

2

3 **Emily Reid and Rob Wilson***

4 *Corresponding author

5

6 **Keywords:** Delta Blue Intensity, Pyrenees, *Pinus uncinata*, summer temperatures

7

8 **Abstract**

9 We explore the potential of the delta Blue Intensity (DBI) parameter as a proxy of past summer temperatures
10 using a well replicated (85 trees) chronology of *Pinus uncinata* from upper treeline in the Spanish Pyrenees.
11 Principal component analysis, correlation response function analysis and Superposed Epoch Analysis show
12 definitively that the DBI data are indistinguishable to other MXD datasets in the region and that DBI expresses
13 a similarly “pure” time-stable climate signal as MXD when compared to their RW counterparts. Calibration r^2
14 values > 0.5 are attainable depending on period used. The signal strength of DBI data is weaker than MXD
15 and behave more like RW data with ca. 19 trees being needed to attain an EPS value > 0.85 . However, as the
16 generation of DBI data is cheaper than MXD, this limitation is not deemed to be a serious issue. This pilot
17 study suggests that robust reconstructions of past summer temperatures could be gained using DBI data at
18 a much-reduced cost than relying on MXD. Future dendroclimatic efforts in the region therefore should focus
19 on the measurement of this parameter and the expansion of the *pinus* ring-density network.

20

21 **Introduction**

22 Tree-rings are invaluable archives of past climate for the late Holocene due to their exact annually
23 resolved dating control (Stokes and Smiley, 1968; Anchukaitis et al., 2012), the generally good understanding
24 of the processes governing tree growth (Fritts, 1976; Körner, 2003; Vaganov et al., 2006; Vaganov et al., 2011;
25 Rossi et al., 2013) and their ability to express a range of different climate variables (Schweingruber, 1988;
26 Jones et al., 2009). Different parameters can be measured from the rings of trees including width, density,
27 wood anatomical properties and stable isotopes (Speer, 2010; Björklund et al. 2019), the variability of which
28 can represent varying climate signals which are often moderated by site ecology. For example, a rough rule
29 of thumb is that the growth of trees growing at high elevation/latitude environments will be temperature
30 limited (Fritts et al., 1965; Kienast et al., 1987; Briffa et al., 2002) while at low elevations/latitudes moisture
31 availability becomes the primary driver of productivity (Fritts, 1976; Cook et al., 2004, 2015). More complex
32 associations exist for stable isotopes (McCarroll and Loader, 2004).

33 For the reconstruction of Northern Hemispheric (NH) summer temperatures, tree-ring records hold
34 particular prominence for the last 1000-2000 years (Masson-Delmotte et al., 2013; PAGES 2k Consortium,
35 2013; Esper et al. 2018). To date, large compilations of temperature sensitive tree-ring data have mostly
36 focussed on both ring-width (RW) and ring-density parameters (Esper et al., 2002; D’Arrigo et al., 2006;
37 Stoffel et al., 2015; Wilson et al., 2016; Anchukaitis et al., 2017) with notable exceptions using only maximum
38 latewood density (MXD - Briffa et al., 2001; Schneider et al., 2015). RW data correlate moderately with
39 summer temperatures (Briffa et al., 2002; Wilson et al., 2016) and generally express strong persistence (i.e.
40 high 1st order autocorrelation) which may impart spectral biases in the resulting local and large-scale
41 temperature estimates (Franke et al., 2013, Lücke et al., 2019). MXD, on the other hand, often matches better
42 the autocorrelation structure of the target summer temperature data (Ljungqvist et al., 2020). In an ideal
43 world, therefore, chronology development (new and updates) should focus on MXD, with RW being used
44 cautiously so long as the spectral properties of the reconstruction matches the instrumental data target. The
45 new generation of tree-ring only NH reconstructions (Schneider et al., 2015; Stoffel et al., 2015; Wilson et al.,
46 2016) represent a substantial improvement on earlier attempts (Briffa et al., 2000; Esper et al., 2002; D’Arrigo
47 et al., 2006). However, despite many studies over the last 20 years definitively detailing that MXD is the more
48 robust parameter (Briffa et al., 2002; Wilson and Luckman, 2003; Esper et al., 2012; Büntgen et al., 2017;
49 Ljungqvist et al., 2020), there has been no community wide strategic plan or investment to update datasets
50 sampled in the 1980s/90s (Schweingruber and Briffa, 1996). Rather, those relatively few important millennial

51 long MXD records that have been developed or updated, represent individual laboratory efforts to create
52 improved regional records (Luckman and Wilson, 2005; Büntgen et al., 2006; Esper et al., 2012; McCarroll et
53 al., 2013; Zhang et al., 2016; Büntgen et al., 2016, 2017; Esper et al., 2019). Presumably, this reflects the
54 relatively small number of tree-ring laboratories with densitometric equipment (Wilson et al., 2014, 2017a)
55 and for this situation to change, a more affordable method is needed that all laboratories can embrace and
56 utilise.

57 Since the initial concept paper (McCarroll et al., 2002), measurement of the intensity of the
58 reflectance of blue light from the latewood of conifer samples (often referred to as Blue Intensity (BI)) has
59 shown great promise as a surrogate and cheaper replacement of MXD (Björklund et al., 2014, 2015; Rydval
60 et al., 2014; Wilson et al., 2014). MXD and BI measure similar wood properties – the relative density of the
61 latewood of conifers - and are well correlated with warm-season temperatures. Most studies that have
62 compared MXD and BI directly show no significant difference between the two parameters (Wilson et al.,
63 2014; Ljungqvist et al., 2020), although in one study BI was found to express temporal instabilities compared
64 to MXD (Kaczka et al., 2018). Despite the ever-expanding number of papers using BI, it must still be seen as
65 an experimental parameter as it has only been utilised on a relatively small number of conifer species (e.g.
66 *Pinus Sylvestris*, Scotland, UK (Rydval et al., 2014), and Scandinavia (Campbell et al., 2007, 2011; Helama et
67 al., 2013; Björklund et al., 2014, 2015; Fuentes et al., 2018); *Picea engelmannii*, the Canadian Rockies, British
68 Columbia, Canada (Wilson et al., 2014); *Picea abies*, Europe (Österreicher et al., 2015; Buras et al., 2018;
69 Kaczka et al., 2018; Rydval et al., 2018); *Abies nordmanniana* in the Northern Caucasus (Dolgova, 2016); *Pinus*
70 *ponderosa*, American SW (Babst et al., 2016); *Pinus cembra*, Austria (Wilson et al., 2017a); *Tsuga mertensiana*
71 (Bong. Carrière), Gulf of Alaska (Wilson et al., 2017b); *Fokienia hodginsii*, central Vietnam (Buckley et al.,
72 2018); *Larix decidua* Mill, European Alps (Arbellay et al., 2018); *Callitropsis nootkatensis* (D. Don) Oerst. ex
73 DP Little, Gulf of Alaska (Wiles et al., 2019); *Picea Glauca*, the Yukon (Wilson et al., 2019)). There is no
74 theoretical reason why BI should not produce similar results for any species from which MXD data have been
75 measured (Björklund et al. 2019). However, the most significant limitation of BI is the fact that it is based on
76 light reflectance. Any colour change on the surface of the wood samples that does not represent year-to-
77 year climate driven latewood cell wall relative density changes (e.g. heartwood/sapwood colour change, or
78 fungal-related discolouration) will impart a potential low frequency bias into the raw measurement data. A
79 proposed method to correct for such biases subtracts the raw latewood minimum BI value from the
80 maximum earlywood BI value (Björklund et al., 2014), producing the so-called Delta BI (DBI) parameter.
81 Compared to standard latewood BI, DBI has only been tested on *Pinus Sylvestris* (Björklund et al., 2014, 2015)
82 and *Tsuga mertensiana* (Wilson et al., 2017b). Herein, we detail a small-scale study that tests DBI on *Pinus*
83 *uncinata* samples from the Spanish Pyrenees by comparing the data with archived MXD chronologies from
84 the surrounding region.

85

86 **Data and Methods**

87 From previous experience working in Scotland, NW North America and the Carpathian Mountains
88 (Rydval et al., 2014, 2018; Wilson et al., 2014, 2017ab, 2019) a single well replicated tree-ring site should
89 allow a robust test of the viability of BI as a climate proxy for any conifer species in a region. This is based on
90 the consistent observation that BI expresses a “purer” summer temperature signal and is less impacted by
91 site ecological (e.g. disturbance) effects than RW. Following this hypothesised approach, we targeted an
92 upper tree-line site in the upper Aranser valley of the Spanish Pyrenees and cored 85 trees of the species
93 *Pinus uncinata* (Figure 1). Previous work in the region has highlighted the greater strength of MXD data as a
94 proxy of summer temperatures over RW (Linán et al., 2012; Büntgen et al., 2008, 2017). For comparative
95 analysis, three archived MXD datasets, within 120 kms of the Aranser valley, were accessed from the
96 International Tree-Ring Databank (ITRDB - Figure 1). These three sites represent similar upper tree-line sites
97 and therefore the trees should express a similar climate response to those at the Aranser study site.

98 The Aranser tree cores were slowly air dried and as this pine species shows a notable colour change
99 from heartwood to sapwood, the samples were immersed in acetone for 72 hours to remove resins in the
100 wood (Rydval et al. 2014). The samples were sanded to 1200 grit and scanned at 3200 dpi resolution using

101 the Silverfast scanning software, calibrated with the IT8.7/2 colour card. Latewood minimum BI and
102 maximum earlywood BI values were measured (see Rydval et al. 2014 for details) using the CooRecorder 8.1
103 software (Cybis 2016 - <http://www.cybis.se/forfun/dendro/index.htm>) and the DBI values calculated
104 (Björklund et al., 2014).

105 Figure 1 shows three example scanned cores after resin extraction treatment. Although resin
106 extractives have theoretically been removed, the wood can still be discoloured by other non-climatic related
107 effects. Samples UAV05 and 15, for example, show dark fungal related staining that was not removed by the
108 acetone treatment. Sample UAV12, despite immersion in acetone, still shows a subtly darker heartwood
109 compared to the sapwood. These colour differences impose systematic biases in the raw reflectance intensity
110 measurements and so the DBI variable will be utilised hereafter as these biases should theoretically be
111 removed or minimised.

112 Based on standardisation experiments from white spruce RW and latewood BI data from the
113 southern Yukon (Wilson et al. 2019), the RW, DBI and MXD data were detrended using an age dependent
114 spline (Melvin et al., 2007) within the signal-free framework (Melvin and Briffa, 2008), while constraining the
115 outermost sections of the fitted function to be non-increasing. This approach appears optimal when
116 compared to commonly used data adaptive methods (i.e. negative exponential or linear functions) and
117 greatly reduces the loss of common mid-frequency variability and any potential warming signal expressed in
118 the tree ring series (Wilson et al., 2019). Chronology signal strength was assessed using the mean-interseries
119 correlation (RBAR) of the detrended series while between-parameter chronology coherence was assessed
120 using correlation matrices and principal component analysis (PCA) over the common 1783-2004 period
121 where replication was greater than 10 series.

122 The climate signal expressed by the RW, DBI and MXD data was examined by calculating monthly and
123 seasonal correlations between the individual chronologies and a regional grid (0-2°E / 42-43°N) of CRUTS4.02
124 mean temperatures (Figure 1 - Harris et al. 2014). The temporal stability of the strongest relationships
125 between the tree-ring variable chronologies and seasonal mean temperatures was explored using running
126 31-year Pearson correlations.

127 Finally, a superposed epoch analysis (SEA) was performed on all the parameter chronologies using
128 the most extreme low index (< -2 STDEV) value years consistent to all three MXD chronologies. These years
129 are inferred to represent the coldest summers over the last 200+ years and the SEA will allow the assessment
130 of not only the likely minimal and lagged response in the RW data (Franke et al., 2013; Lücke et al., 2019),
131 but also how well the DBI data express these cold summers. For the SEA, the 15 years after each identified
132 cold year are transformed to z-scores with respect to the mean and standard deviation of the preceding 5
133 years and the varying epoch segments averaged to derive a mean change in z-score values.

134

135 **Results and Discussion**

136 The between-chronology coherence is stronger for MXD/DBI than RW with a mean inter-series
137 correlation of 0.78 compared to 0.57 (Figure 2A+B). The Aranser RW chronology correlates with the other
138 sites with a range of 0.48 – 0.70 (mean $r = 0.61$), while the DBI data express a range of 0.75 – 0.82 (mean $r =$
139 0.77) with the MXD data. This stronger common signal of the MXD/DBI data is further highlighted by the PCA
140 with the MXD/DBI chronologies loading on PC1 (explaining 57.3% of the overall variance) while the RW data
141 load on PC2 (explaining just 19.5% of the variance – Figure 2C). These results clearly highlight the “purer”
142 common signal expressed by the MXD/DBI chronologies compared to RW, which is presumably more
143 influenced by site specific varying ecological factors (Björklund et al., 2014; Rydval et al., 2014, 2018; Wilson
144 et al., 2014, 2017a). Importantly, the DBI data express a very similar signal to the MXD data and qualitatively,
145 despite the discolouration issues noted in some samples (Figure 1), the DBI chronology does not deviate in
146 any significant way from the MXD series (Figure 2B).

147 The chronology signal strength, measured by the mean inter-series correlation (RBAR), is weaker for
148 the RW data (0.23 ± 0.03 STDEV) than MXD (0.34 ± 0.06 STDEV). Previous studies have detailed the weaker
149 signal strength in BI-based parameters compared to MXD (Rydval et al., 2014; Kaczka et al., 2018; Wilson et
150 al., 2014, 2017a) and our results are no different, with DBI expressing similar signal strength properties to

151 RW (RBAR = 0.23 - Figure 2D). The implications of these results are that on average, for MXD data, ca. 11
152 trees are needed to attain an Expressed Population Signal of 0.85 (Wigley et al., 1984; Wilson and Elling,
153 2004) while ca. 19 trees are needed for RW and DBI.

154 Despite the RW and MXD/DBI data expressing enough unique variance to identify two eigenvectors
155 in the PCA (Figures 2C), the correlations of the RW and MXD/DBI chronologies with mean monthly and
156 seasonal temperature are broadly similar (Figure 3) although RW expresses an overall weaker climate signal.
157 Over the 1901-2004 period, the RW data for all 4 sites correlate most strongly with May-August temperatures
158 with a range of 0.42 - 0.54 (Figure 3A). For MXD, correlations are highest with May-September temperatures
159 - the range being 0.59 – 0.69, while DBI correlates at 0.62 (Figure 3B). The temporal stability of the climate
160 signal in the RW data is poor (Figure 3C) with highest correlations noted in recent decades, but most of the
161 RW sites hover around or below significance for most of the 20th century, although one (SPA1069) notably
162 drops to negative values through this period. The climate/parameter relationship of the MXD and DBI data
163 is much more stable, although, as noted by Büntgen et al. (2017), post 1950 correlations are marginally - but
164 not significantly - stronger (Figure 3D). Büntgen et al. (2017) calibrated against a split season of May-June
165 and August-September and attained a correlation of 0.72 over the 1950-2014 period. In our analyses herein,
166 all chronology correlations with July temperatures for both RW and MXD/DBI are significant (Figure 3A+B)
167 and we see no justification for the use of the split season. Correlations with the full May-September season
168 are in fact more temporally stable, with the MXD data for the 1901-1949 and 1950-2004 periods expressing
169 a mean correlation of 0.65 (\pm 0.08 STDEV) and 0.69 (\pm 0.12 STDEV), respectively (see inset table in Figure
170 3D). At the individual site level, FRAN042 and FRAN043 actually express marginally stronger correlations for
171 the earlier period. The DBI chronology correlates at 0.68 and 0.73 for both periods. For the split May-
172 June/August-September season, the equivalent correlations for MXD and DBI are 0.61 (\pm 0.07 STDEV) and
173 0.65 (\pm 0.11 STDEV), and 0.64 and 0.78. However, regardless of which season is deemed appropriate, the
174 DBI results are not significantly different to those of the MXD data.

175 As the Aranser trees and those from the other three sites were sampled near upper treeline, the
176 positive correlations with summer temperatures are not unexpected (Figure 3). It is well known that MXD
177 expresses a strong correlation with summer temperatures and it is the tree-ring parameter of choice if one
178 wants to explore the summer temperature response to significant major volcanic eruptions (Anchukaitis et
179 al., 2012; D'Arrigo et al. 2013; Schneider et al., 2015). To assess whether DBI may also portray similar
180 properties to MXD, significant inferred cold years were identified using annual values 2 standard deviations
181 below the 1783-2004 mean across all three MXD chronologies. These years - 1809, 1816, 1829, 1835, 1850,
182 1910, 1939, 1963 and 1972 – were utilised in a Superposed Epoch Analysis (SEA) to identify the mean
183 response of the RW and DBI data to extreme inferred cold summers. Three of these years (1809, 1816 and
184 1835) are well known cool summers related to major tropical eruptions (Wilson et al., 2016). The SEA results
185 (Figure 4) show that the DBI data express the same mean response cooling of ca. 2 standard deviations as
186 the MXD sites. The RW chronologies, on the other hand, show a complex, more dampened decrease of only
187 ca. 1 standard deviation one year later than the MXD/DBI data. SEA analyses comparing RW and MXD at
188 regional and hemispheric scales show similar differences between the two parameters (Anchukaitis et al.,
189 2012; D'Arrigo et al. 2013; Wilson et al., 2016). Measurements of 1st order autocorrelation (AC) are often
190 used to highlight potential autoregressive biological memory issues of RW when compared to MXD (Franke
191 et al., 2013; Lücke et al., 2019). The mean 1st order AC of the four RW chronologies (1901-2004) is 0.44 (\pm
192 0.09 STDEV – Figure 2E) while for the MXD data it is 0.18 (\pm 0.08 STDEV). The DBI data again sit within this
193 MXD range with a mean 1st order AC of 0.24. Initially, these results would sit well with the SEA results in that
194 the RW data express a dampened lagged response. However, the 1st order AC for both the MJJA and MJJAS
195 mean temperature seasons is 0.36 suggesting that caution is needed in assuming that ring density
196 parameters reflect the spectral properties of the instrumental data, as they may in fact be too white.

197 198 **Concluding Remarks**

199 In this study, we have measured DBI data from a single well replicated *Pinus uncinata* site at upper
200 treeline in the Spanish Pyrenees and compared the chronology properties with MXD data from similar sites

201 within 120 kms. Despite heartwood/sapwood and fungal-related discolouration (Figure 1), the DBI data
202 appear to minimise the colour biases that would be expressed by the latewood BI data, and no significant
203 trend differences are noted between the MXD and DBI chronologies (Figure 2B). Principal component
204 analysis, correlation response function analysis and Superposed Epoch Analysis show definitively that the DBI
205 data are indistinguishable to the MXD data and that DBI expresses a similarly “pure” climate signal as MXD
206 when compared to their RW counterparts (Björklund et al., 2014; Rydval et al., 2014, 2018; Wilson et al.,
207 2014, 2017a). In many respects, these results are not surprising as both DBI and MXD measure similar wood
208 properties – the relative density of the latewood of conifers. However, the number of studies utilising DBI
209 are still small (Björklund et al., 2014, 2015; Wilson et al., 2017b) and it cannot be guaranteed that this
210 parameter will always minimise discolouration bias. The only property of the DBI data significantly different
211 to MXD was the chronology signal strength (RBAR) where the DBI data express a weaker between-tree
212 common signal and behave more like RW data with ca. 19 trees being needed to attain an EPS value > 0.85
213 (Figure 2D). As the generation of latewood BI or DBI data is so much cheaper than MXD, this limitation is not
214 deemed to be a serious issue.

215 This paper represents the latest of only a small number of studies (Björklund et al., 2014, 2015;
216 Wilson et al., 2017b) examining the potential of DBI for dendroclimatology. Our results, despite utilising data
217 from only one location, strongly suggest that the added expense of measuring MXD data is likely not needed
218 in this region and substantial improvement in calibration and validation would be gained by expanding the
219 *pinus* DBI network across the Pyrenees region (see Linán et al., 2012) rather than focussing on a single
220 location with very high replication (Büntgen et al., 2017). 30-40 living trees would be adequate for each site,
221 but for the period prior to 1700, preserved non-living snag, sub-fossil or historical (Wilson et al. 2004)
222 material would be needed to significantly extend the chronologies back in time. Sites with profuse amounts
223 of surface dead snag material (Büntgen et al., 2017) would be vital, as well as exploring the potential of
224 finding high elevation lakes where stem material may be preserved in the near-shore sediments. However,
225 the darker nature of preserved dead surface or sub-fossil wood could be a major hinderance, due to the
226 discolouration bias, for the use of reflectance-based parameters for dendroclimatology. Some studies have
227 overcome these colour biases effectively by either adjusting the BI data using contrast adjustments
228 (Björklund et al., 2015; Fuentes et al., 2018) or employing a band-pass approach where the low frequency
229 signal is derived from the RW data and the high frequency is driven by the BI data (Rydval et al., 2017;). Much
230 more experimentation is needed, however, before the utilisation of BI and related parameters, measured
231 from preserved snag, sub-fossil or historical material, can be deemed as trustworthy. It’s not inconceivable
232 that wood anatomical approaches may, in the end, provide the true non-biased estimate of relative wood
233 density in tree-ring series (Björklund et al., 2020).

234
235

236 **Acknowledgments**

237 This paper is dedicated to Fritz Schweingruber who passed away while this manuscript was being finalised.
238 He was an inspiration to all dendrochronologists and was integral in the exploration of conifer tree-ring
239 density parameters for dendroclimatology in the 1970s. The development of Blue Intensity over the last
240 decade benefitted greatly from Fritz’ experience and insight. He will be sorely missed. Many thanks to Cheryl
241 Wood and Hannah Frith for measurement of much of the material utilised in this study and Jesper Björklund
242 for his kind but robust review.

243

244 **References**

245

246 Arbella, E., Jarvis, I., Chavardès, R.D., Daniels, L.D. and Stoffel, M., 2018. Tree-ring proxies of larch bud moth
247 defoliation: latewood width and blue intensity are more precise than tree-ring width. *Tree physiology* 38(8),
248 1237-1245.

249

250 Anchukaitis, K., Breitenmoser, P., Briffa, K., Buchwal, A., Büntgen, U., Cook, E., D'Arrigo, R., Esper, J., Evans,
251 M., Frank, D., Grudd, H., Gunnarson, B., Hughes, M., Kirdyanov, A., Körner, C., Krusic, P., Luckman, B., Melvin,
252 T., Salzer, M., Shashkin, A., Timmreck, C., Vaganov, E., Wilson, R., 2012. Tree rings and volcanic cooling.
253 Nature Geoscience 5, 836–837. doi:10.1038/ngeo1645
254

255 Anchukaitis, K.J., Wilson, R., Briffa, K., Büntgen, U., Cook, E.R., D'Arrigo, R.D., Davi, N., Esper, J., Frank, D.,
256 Gunnarson, B., Hegerl, G., Helama, S., Klesse, S., Krusic, P.J., Linderholm, H., Myglan, V., Osborn, T.J., Peng,
257 Z., Rydval, M., Schneider, L., Schurer, A., Wiles, G., Zorita, A., 2017. Last millennium Northern Hemisphere
258 summer temperatures from tree rings: Part II: spatially resolved reconstructions. Quaternary Science Reviews
259 163, 1-22. doi: 10.1016/j.quascirev.2017.02.020
260

261 Babst, F., Wright, W.E., Szejnjer, P., Wells, L., Belmecheri, S., Monson, R.K., 2016. Blue intensity parameters
262 derived from Ponderosa pine tree rings characterize intra-annual density fluctuations and reveal seasonally
263 divergent water limitations. Trees 30(4), 1403-1415.
264

265 Björklund, J.A., Gunnarson, B.E., Seftigen, K., Esper, J., Linderholm, H.W., 2014. Blue intensity and density
266 from northern Fennoscandian tree rings, exploring the potential to improve summer temperature
267 reconstructions with earlywood information. Climate of the Past 10(2), 877-885.
268

269 Björklund, J., Gunnarson, B.E., Seftigen, K., Zhang, P., Linderholm, H.W., 2015. Using adjusted blue intensity
270 data to attain high-quality summer temperature information: a case study from Central Scandinavia. The
271 Holocene 25(3), 547-556.
272

273 Björklund, J., Arx, G., Nievergelt, D., Wilson, R., Van den Bulcke, J., Günther, B., Loader, N.J., Rydval, M., Fonti,
274 P., Scharnweber, T., Andreu-Hayles, L., Büntgen, U., D'Arrigo, R., Davi, N., De Mil, T., Esper, J., Gärtner, H.,
275 Geary, J., Gunnarson, B.E., Hartl, C., Hevia, A., Song, H., Janecka, K., Kaczka, R.J., Kirdyanov, A.V., Kochbeck,
276 M., Liu, Y., Meko, M., Mundo, I., Nicolussi, K., Oelkers, R., Pichler, T., Sánchez-Salguero, R., Schneider, L.,
277 Schweingruber, F., Timonen, M., Trouet, V., Van Acker, J., Verstege, A., Villalba, R., Wilmking, M. and Frank,
278 D., 2019. Scientific Merits and Analytical Challenges of Tree-Ring Densitometry. Reviews of Geophysics, art.
279 2019RG000642, doi:10.1029/2019rg000642.
280

281 Björklund, J., Seftigen, K., Fonti, P., Nievergelt, D. and von Arx, G., 2020. Dendroclimatic potential of
282 dendroanatomy in temperature-sensitive *Pinus sylvestris*. Dendrochronologia, 60, p.125673.
283

284 Briffa, K.R., Osborn, T.J., Schweingruber, F.H., Harris, I.C., Jones, P.D., Shiyatov, S.G., Vaganov, E.A., 2001.
285 Low-frequency temperature variations from a northern tree ring density network. Journal of Geophysical
286 Research: Atmospheres 106(D3), 2929-2941.
287

288 Briffa, K.R., Osborn, T.J., Schweingruber, F.H., Jones, P.D., Shiyatov, S.G., Vaganov, E.A., 2002. Tree-ring width
289 and density data around the Northern Hemisphere: Part 1, local and regional climate signals. The Holocene
290 12(6), 737-757.
291

292 Buckley, B.M., Hansen, K.G., Griffin, K.L., Schmiege, S., Oelkers, R., D'Arrigo, R.D., Stahle, D.K., Davi, N.,
293 Nguyen, T.Q.T., Le, C.N., Wilson, R.J., 2018. Blue intensity from a tropical conifer's annual rings for climate
294 reconstruction: An ecophysiological perspective. Dendrochronologia 50, 10-22.
295

296 Buras, A., Spyt, B., Janecka, K., Kaczka, R., 2018. Divergent growth of Norway spruce on Babia Góra Mountain
297 in the western Carpathians. Dendrochronologia 50, 33-43.
298

299 Büntgen, U., Frank, D.C., Nievergelt, D., Esper, J., 2006. Summer temperature variations in the European Alps,
300 AD 755–2004. *Journal of Climate* 19(21), 5606-5623.
301

302 Büntgen, U., Myglan, V.S., Ljungqvist, F.C., McCormick, M., Di Cosmo, N., Sigl, M., Jungclaus, J., Wagner, S.,
303 Krusic, P.J., Esper, J., Kaplan, J.O., 2016. Cooling and societal change during the Late Antique Little Ice Age
304 from 536 to around 660 AD. *Nature Geoscience* 9(3), 231.
305

306 Büntgen, U., Krusic, P., Verstege, A., Sangüesa-Barreda, G., Wagner, S., Camarero, J.J., Zorita, E., Ljungqvist,
307 F.C., Konter, O., Oppenheimer, C., Tegel, W., Gärtner, H., Cherubini, P., Reinig, F., Esper, J., 2017. New tree-
308 ring evidence from the Pyrenees reveals western Mediterranean climate variability since medieval times.
309 *Journal of Climate* 30, 5295-5318.
310

311 Campbell, R., McCarroll, D., Loader, N.J., Grudd, H., Robertson, I., Jalkanen, R., 2007. Blue intensity in *Pinus*
312 *sylvestris* tree-rings: developing a new palaeoclimate proxy. *The Holocene* 17(6), 821-828.
313

314 Campbell, R., McCarroll, D., Robertson, I., Loader, N.J., Grudd, H., Gunnarson, B., 2011. Blue intensity in *Pinus*
315 *sylvestris* tree rings: a manual for a new palaeoclimate proxy. *Tree-Ring Research* 67(2), 127-135.
316

317 Cook, E.R., Woodhouse, C.A., Eakin, C.M., Meko, D.M., Stahle, D.W., 2004. Long-term aridity changes in the
318 western United States. *Science* 306(5698), 1015-1018.
319

320 Cook, E.R., Seager, R., Kushnir, Y., Briffa, K.R., Büntgen, U., Frank, D., Krusic, P.J., Tegel, W., Van der Schrier,
321 G., Andreu-Hayles, L., Baillie, M., Baittinger, C., Bleicher, N., Bonde, N., Brown, D., Career, M., Cooper, R.,
322 Cufar, K., Dittmar, C., Esper, J., Griggs, C., Gunnarson, B., Günther, B., Gutierrez, E., Haneca, K., Helama, S.,
323 Herzig, F., Heussner, K-U., Hofmann, J., Janda, P., Kontic, R., Köse, N., Kyncl, T., Levanic, T., Linderholm, H.,
324 Manning, S., Melvin, T.M., Miles, D., Neuwirth, B., Nicolussi, K., Nola, P., Panayotov, M., Popa, I., Rothe, A.,
325 Seftigen, K., Seim, A., Svarva, H., Svoboda, M., Thun, T., Timonen, M., Touchan, R., Trotsiuk, V., Trouet, V.,
326 Walder, F., Wazny, T., Wilson, R., Zang, C., 2015. Old World megadroughts and pluvials during the Common
327 Era. *Science Advances* 1, e1500561.
328

329 D'Arrigo, R., Wilson, R., Jacoby, G., 2006. On the long-term context for late twentieth century warming.
330 *Journal of Geophysical Research: Atmospheres* 111(D3).
331

332 D'Arrigo, R., Wilson, R. and Anchukaitis, K.J., 2013. Volcanic cooling signal in tree ring temperature records
333 for the past millennium. *Journal of Geophysical Research: Atmospheres*, 118(16), pp.9000-9010.
334

335 Dolgova, E., 2016. June–September temperature reconstruction in the Northern Caucasus based on blue
336 intensity data. *Dendrochronologia* 39, 17-23.
337

338 Esper, J., Cook, E.R., Schweingruber, F.H., 2002. Low-frequency signals in long tree-ring chronologies for
339 reconstructing past temperature variability. *Science* 295(5563), 2250-2253.
340

341 Esper, J., Frank, D.C., Timonen, M., Zorita, E., Wilson, R.J., Luterbacher, J., Holzkämper, S., Fischer, N., Wagner,
342 S., Nievergelt, D., Verstege, A., 2012. Orbital forcing of tree-ring data. *Nature Climate Change* 2(12), 862.
343

344 Esper, J., George, S.S., Anchukaitis, K., D'Arrigo, R., Ljungqvist, F.C., Luterbacher, J., Schneider, L., Stoffel, M.,
345 Wilson, R. and Büntgen, U., 2018. Large-scale, millennial-length temperature reconstructions from tree-rings.
346 *Dendrochronologia*, 50, pp.81-90.
347

348 Esper, J., Klippel, L., Krusic, P.J., Konter, O., Raible, C.C., Xoplaki, E., Luterbacher, J., Büntgen, U., 2019. Eastern
349 Mediterranean summer temperatures since 730 CE from Mt. Smolikas tree-ring densities. *Climate Dynamics*,
350 1-16.
351

352 Franke, J., Frank, D., Raible, C.C., Esper, J., Brönnimann, S., 2013. Spectral biases in tree-ring climate proxies.
353 *Nature Climate Change* 3(4), 360.
354

355 Fritts, H.C., Smith, D.G., Cardis, J.W., Budelsky, C.A., 1965. Tree-ring characteristics along a vegetation
356 gradient in northern Arizona. *Ecology* 46(4), 393-401.
357

358 Fritts, H.C., 1976. *Tree Rings and Climate*. Academic Press. San Diego, Calif.
359

360 Fuentes, M., Salo, R., Björklund, J., Seftigen, K., Zhang, P., Gunnarson, B., Aravena, J.C., Linderholm, H.W.,
361 2018. A 970-year-long summer temperature reconstruction from Rogen, west-central Sweden, based on blue
362 intensity from tree rings. *The Holocene* 28(2), 254-266.
363

364 Harris, I.P., Jones, P.D., Osborn, T.J. and Lister, D.H., 2014. Updated high-resolution grids of monthly climatic
365 observations—the CRU TS3. 10 Dataset. *International journal of climatology*, 34(3), pp.623-642.
366

367 Helama, S., Arentoft, B.W., Collin-Haubensak, O., Hyslop, M.D., Brandstrup, C.K., Mäkelä, H.M., Tian, Q.
368 Wilson, R., 2013. Dendroclimatic signals deduced from riparian versus upland forest interior pines in North
369 Karelia, Finland. *Ecological Research* 28(6), 1019-1028.
370

371 Jones, P., Briffa, K., Osborn, T., Lough, J., van Ommen, T., Vinther, B., Luterbacher, J., Wahl, E., Zwiets, F.,
372 Mann, M., Schmidt, G., Ammann, C., Buckley, B., Cobb, K., Esper, J., Goussé, H., Graham, N., Jansen, E., Kiefer,
373 T., Kull, C., Küttel, M., Mosley Thompson, E., Overpeck, J., Riedwyl, N., Schulz, M., Tudhope, A., Villalba, R.,
374 Wanner, H., Wolff, E., Xoplaki, E., 2009. High-resolution palaeoclimatology of the last millennium: a review
375 of current status and future prospects. *Holocene* 19, 3-49.
376

377 Kaczka, R.J., Spyt, B., Janecka, K., Beil, I., Büntgen, U., Scharnweber, T., Nievergelt, D., Wilmking, M., 2018.
378 Different maximum latewood density and blue intensity measurements techniques reveal similar results.
379 *Dendrochronologia* 49, 94-101.
380

381 Kienast, F., Schweingruber, F.H., Bräker, O.U. and Schär, E., 1987. Tree-ring studies on conifers along
382 ecological gradients and the potential of single-year analyses. *Canadian Journal of Forest Research* 17(7),
383 683-696.
384

385 Körner, C., 2003. Carbon limitation in trees. *Journal of Ecology* 91(1), 4-17.
386

387 Linán, I.D., Büntgen, U., González-Rouco, F., Zorita, E., Montávez, J.P., Gómez-Navarro, J.J., Brunet, M.,
388 Heinrich, I., Helle, G., Gutiérrez, E., 2012. Estimating 750 years of temperature variations and uncertainties
389 in the Pyrenees by tree ring reconstructions and climate simulations. *Climate of the Past* 8(3), 919-933.
390

391 Ljungqvist, F.C., Thejll, P., Björklund, J., Gunnarson, B.E., Piermattei, A., Rydval, M., Seftigen, K., Støve, B.,
392 Büntgen, U., 2020. Assessing non-linearity in European temperature-sensitive tree-ring data.
393 *Dendrochronologia* 59, 125652.
394

395 Lücke, L.J., Hegerl, G.C., Schurer, A.P., Wilson, R., 2019. Effects of memory biases on variability of temperature
396 reconstructions. *Journal of Climate* 32(24), 8713-8731.
397

398 Luckman, B.H., Wilson, R.J.S., 2005. Summer temperatures in the Canadian Rockies during the last
399 millennium: a revised record. *Climate Dynamics* 24(2-3), 131-144.
400

401 Masson-Delmotte, V., Schulz, M., Abe-Ouchi, A., Beer, J., Ganopolski, A., Gonzalez Rouco, J.F., Jansen, E.,
402 Lambeck, K., Luterbacher, J., Naish, T., Osborn, T., Otto-Bliesner, B., Quinn, T., Ramesh, R., Rojas, M., Shao,
403 X., Timmermann, A., 2013. Information from paleoclimate archives, in: Stocker, T.F., Qin, D., Plattner, G.K.,
404 Tignor, M., Allen, S.K., Boschung, J., Nauels, A., Xia, Y., Bex, V., Midgley, P.M. (Eds.), *Climate Change 2013: the*
405 *Physical Science Basis. Contribution of Working Group I to the Fifth Assessment Report of the*
406 *Intergovernmental Panel on Climate Change. Cambridge University Press, Cambridge, United Kingdom and*
407 *New York, NY, USA, pp. 383-464.*
408

409 McCarroll, D., Pettigrew, E., Luckman, A., Guibal, F., Edouard, J.L., 2002. Blue reflectance provides a surrogate
410 for latewood density of high-latitude pine tree rings. *Arctic, Antarctic, and Alpine Research* 34(4), 450-453.
411

412 McCarroll, D., Loader, N.J., 2004. Stable isotopes in tree rings. *Quaternary Science Reviews* 23(7-8), 771-801.
413

414 McCarroll, D., Loader, N.J., Jalkanen, R., Gagen, M.H., Grudd, H., Gunnarson, B.E., Kirchhefer, A.J., Friedrich,
415 M., Linderholm, H.W., Lindholm, M., Boettger, T., Los, S.O., Remmele, S., Kononov, Y.M., Yamazaki, Y.H.,
416 Young, G.H.F., Zorita, E., 2013. A 1200-year multiproxy record of tree growth and summer temperature at
417 the northern pine forest limit of Europe. *Holocene* 23(4), 471-484.
418

419 Melvin, T.M., Briffa, K.R., Nicolussi, K., Grabner, M., 2007. Time-varying-response smoothing.
420 *Dendrochronologia* 25(1), 65-69.
421

422 Melvin, T.M., Briffa, K.R., 2008. A "signal-free" approach to dendroclimatic standardisation.
423 *Dendrochronologia* 26(2), 71-86.
424

425 Österreicher, A., Weber, G., Leuenberger, M., Nicolussi, K., 2015. Exploring blue intensity-comparison of blue
426 intensity and MXD data from Alpine spruce trees. *TRACE—Tree Rings in Archaeology, Climatology and Ecology*
427 13, 56-61.
428

429 PAGES 2k Consortium, 2013. Continental-scale temperature variability during the past two millennia. *Nature*
430 *Geoscience* 6, 339-346.
431

432 Rossi, S., Anfodillo, T., Čufar, K., Cuny, H.E., Deslauriers, A., Fonti, P., Frank, D., Gričar, J., Gruber, A., King,
433 G.M., Krause, C., 2013. A meta-analysis of cambium phenology and growth: linear and non-linear patterns in
434 conifers of the northern hemisphere. *Annals of Botany* 112(9), 1911-1920.
435

436 Rydval, M., Larsson, L.Å., McGlynn, L., Gunnarson, B.E., Loader, N.J., Young, G.H., Wilson, R., 2014. Blue
437 intensity for dendroclimatology: should we have the blues? *Experiments from Scotland. Dendrochronologia*
438 32(3), 191-204.
439

440 Rydval, M., Loader, N.J., Gunnarson, B.E., Druckenbrod, D.L., Linderholm, H.W., Moreton, S.G., Wood, C.V.
441 and Wilson, R., 2017. Reconstructing 800 years of summer temperatures in Scotland from tree rings. *Climate*
442 *Dynamics*, 49(9-10), pp.2951-2974.
443

444 Rydval, M., Druckenbrod, D.L., Svoboda, M., Trotsiuk, V., Janda, P., Mikoláš, M., Čada, V., Bače, R., Teodosiu,
445 M., Wilson, R., 2018. Influence of sampling and disturbance history on climatic sensitivity of temperature-
446 limited conifers. *The Holocene* 28(10), 1574-1587.
447

448 Schneider, L., Smerdon, J.E., Büntgen, U., Wilson, R.J., Myglan, V.S., Kirilyanov, A.V., Esper, J., 2015. Revising
449 midlatitude summer temperatures back to AD 600 based on a wood density network. *Geophysical Research*
450 *Letters* 42(11), 4556-4562.

451

452 Schweingruber, F.H., 1988. *Tree rings: basics and applications of dendrochronology*. Springer Science &
453 Business Media.

454

455 Schweingruber, F.H., Briffa, K.R., 1996. Tree-ring density networks for climate reconstruction in: Jones P.D.,
456 Bradley R.S., Jouzel J. (Eds.), *Climatic variations and forcing mechanisms of the last 2000 years*. Springer,
457 Berlin, Heidelberg, pp. 43-66.

458

459 Speer, J.H., 2010. *Fundamentals of tree-ring research*. University of Arizona Press.

460

461 Stoffel, M., Khodri, M., Corona, C., Guillet, S., Poulain, V., Bekki, S., Guiot, J., Luckman, B.H., Oppenheimer,
462 C., Lebas, N., Beniston, M., 2015. Estimates of volcanic-induced cooling in the Northern Hemisphere over the
463 past 1,500 years. *Nature Geoscience* 8(10), 784.

464

465 Stokes, M.A., Smiley, T.L., 1968. *An Introduction to Tree Ring Dating*. University of Chicago Press. 73p.

466

467 Vaganov, E.A., Hughes, M.K., Shashkin, A.V., 2006. *Growth dynamics of conifer tree rings: images of past and*
468 *future environments*. Ecological studies 183. Springer Science & Business Media, Berlin.

469

470 Vaganov, E.A., Anchukaitis, K.J., Evans, M.N., 2011. How well understood are the processes that create
471 dendroclimatic records? A mechanistic model of the climatic control on conifer tree-ring growth dynamics
472 in: Hughes M., Swetnam T., Diaz H. (Eds.), *Dendroclimatology* 11. Springer, Dordrecht, pp. 37-75.

473

474 Wigley, T.M., Briffa, K.R., Jones, P.D., 1984. On the average value of correlated time series, with applications
475 in dendroclimatology and hydrometeorology. *Journal of Climate and Applied Meteorology* 23(2), 201-213.

476

477 Wiles, G.C., Charlton, J., Wilson, R.J., D'Arrigo, R.D., Buma, B., Krapek, J., Gaglioti, B.V., Wiesenberg, N.,
478 Oelkers, R., 2019. Yellow-cedar blue intensity tree-ring chronologies as records of climate in Juneau, Alaska,
479 USA. *Canadian Journal of Forest Research* 49(12), 1483-1492.

480

481 Wilson, R.J., Luckman, B.H., 2003. Dendroclimatic reconstruction of maximum summer temperatures from
482 upper treeline sites in Interior British Columbia, Canada. *The Holocene* 13(6), 851-861.

483

484 Wilson, R., Elling, W., 2004. Temporal instability in tree-growth/climate response in the Lower Bavarian
485 Forest region: implications for dendroclimatic reconstruction. *Trees* 18(1), 19-28.

486

487 Wilson, R.J., Esper, J. and Luckman, B.H., 2004. Utilising historical tree-ring data for dendroclimatology: a case
488 study from the Bavarian Forest, Germany. *Dendrochronologia*, 21(2), pp.53-68.

489

490 Wilson, R.J.S, Rao, R., Rydval, M., Wood, C., Larsson, L.-A., Luckman, B.H. 2014. Blue Intensity for
491 Dendroclimatology: The BC Blues: A Case Study from British Columbia Canada. *The Holocene* 24 (11), 1428-
492 1438.

493

494 Wilson, R., Anchukaitis, K., Briffa, K., Büntgen, U., Cook, E., D'Arrigo, R., Davi, N., Esper, J., Frank, D.,
495 Gunnarson, B., Hegerl, G., Helema, S., Klesse, S., Krusic, P., Linderholm, H.W., Myglan, V., Osborn, T., Rydval,
496 M., Schneider, L., Schurer, A., Wiles, G., Zhang, P., Zorita, E., 2016. Last millennium Northern Hemisphere
497 summer temperatures from tree rings: Part I: the long term context. *Quaternary Science Reviews* 134, 1-18.

498

499

500 Wilson, R., Wilson, D., Rydval, M., Crone, A., Büntgen, U., Clark, S., Ehmer, J., Forbes, E., Fuentes, M.,
501 Gunnarson, B.E., Linderholm, H., Nicolussi, K., Wood, C., Mills, C. 2017a. Facilitating tree-ring dating of
502 historic conifer timbers using Blue Intensity. *Journal of Archaeological Science* 78, 99-111.

503

504 Wilson, R., D'Arrigo, R., Andreu-Hayles, L., Oelkers, R., Wiles, G., Anchukaitis, K., Davi, N., 2017b. Experiments
505 based on blue intensity for reconstructing North Pacific temperatures along the Gulf of Alaska. *Climate of the*
506 *Past* 13(8), 1007-1022.

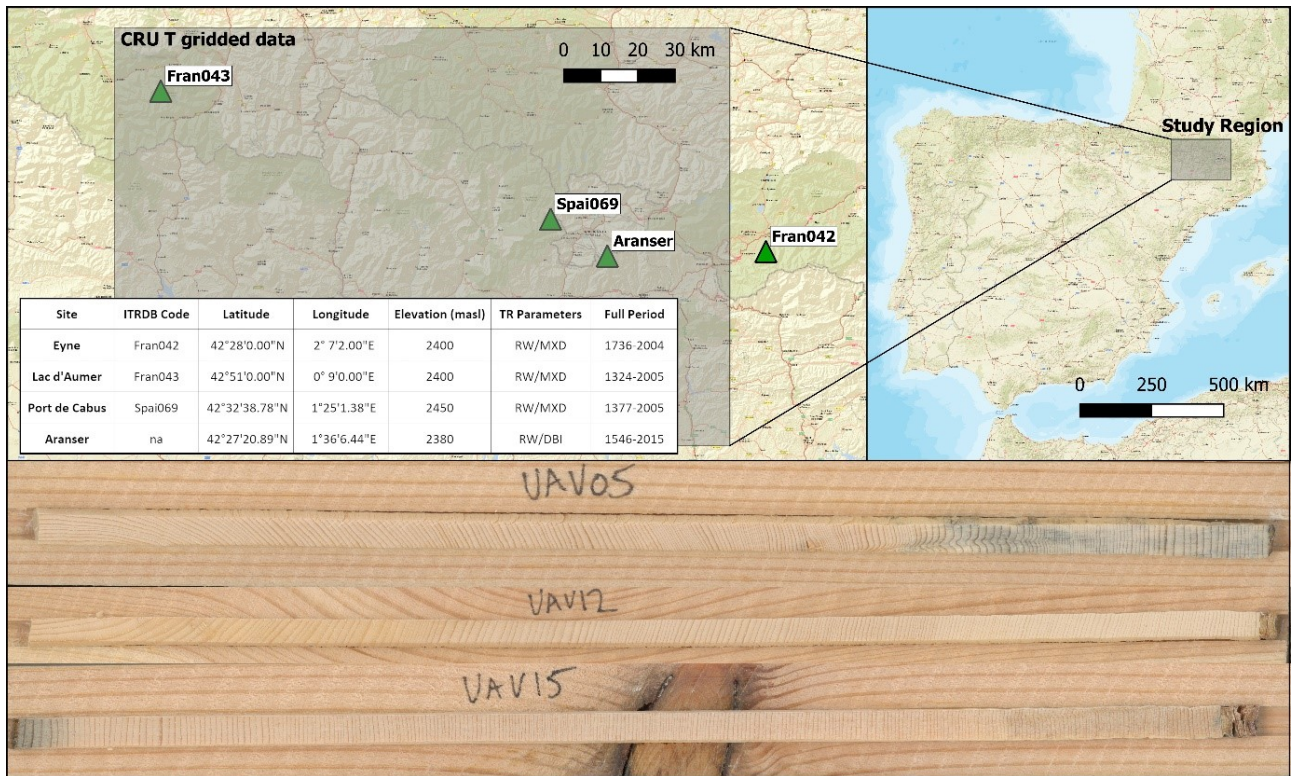
507

508 Wilson, R., Anchukaitis, K., Andreu-Hayles, L., Cook, E., D'Arrigo, R., Davi, N., Haberbauer, L., Krusic, P.,
509 Luckman, B., Morimoto, D., Oelkers, R., 2019. Improved dendroclimatic calibration using blue intensity in the
510 southern Yukon. *The Holocene* 29(11), 1817-1830.

511

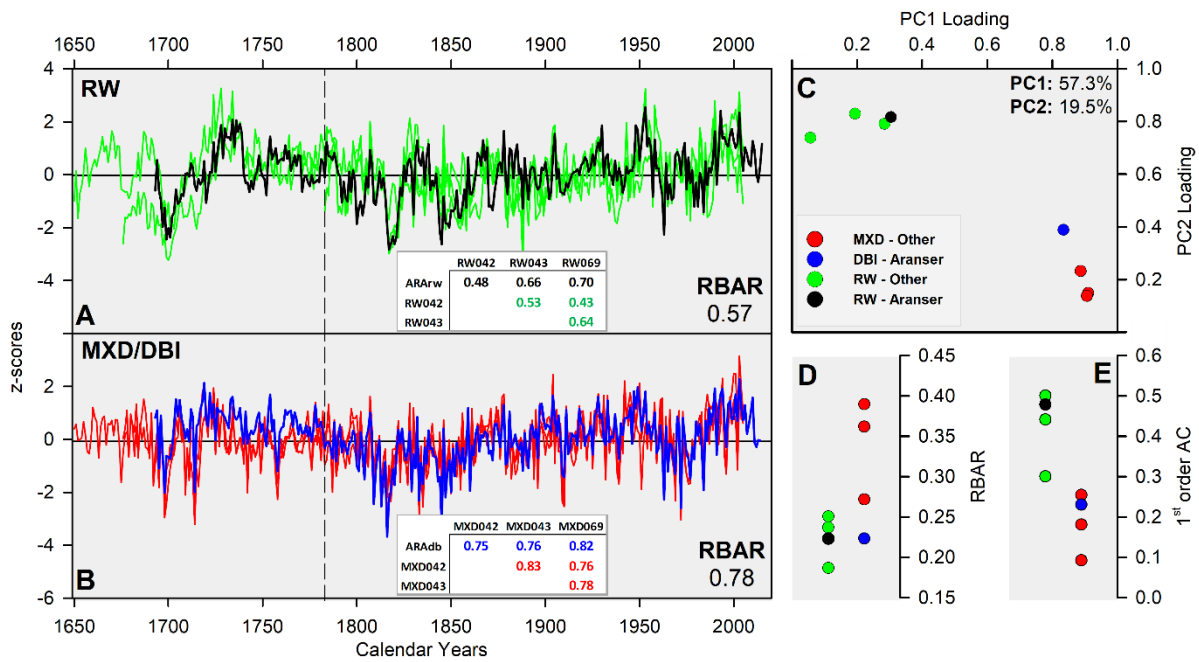
512 Zhang, P., Linderholm, H.W., Gunnarson, B.E., Björklund, J., Chen, D., 2016. 1200 years of warm-season
513 temperature variability in central Scandinavia inferred from tree-ring density. *Climate of the Past* 12(6), 1297-
514 1312.

515



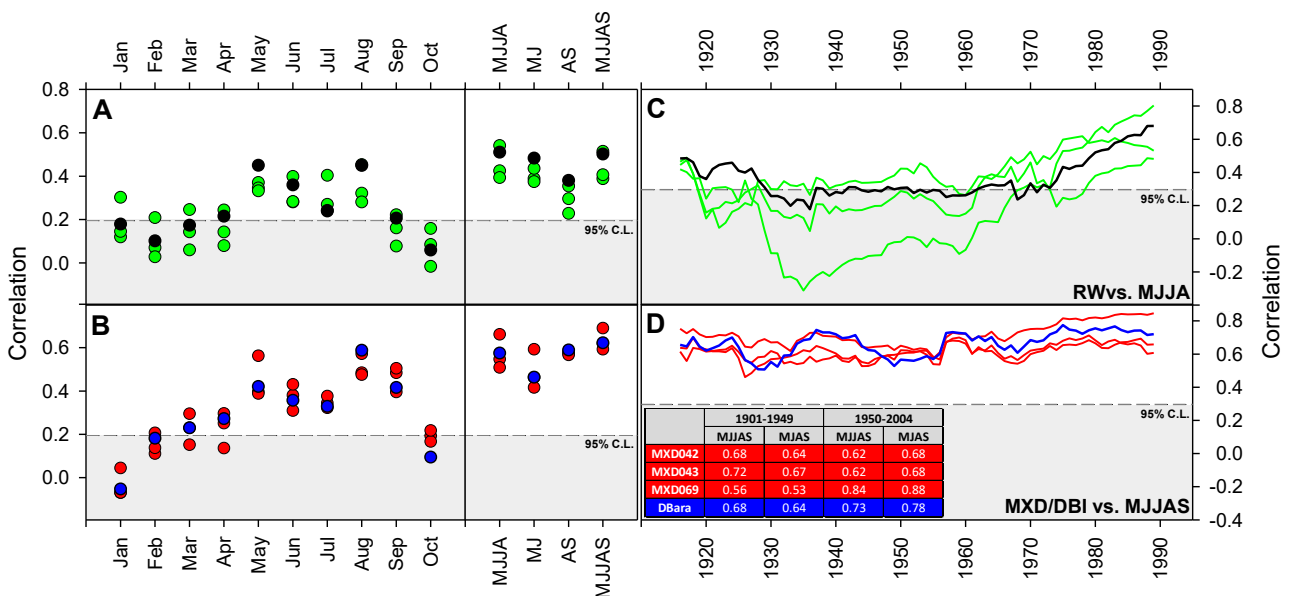
516
517
518
519
520
521
522
523
524

Figure 1: Upper: Location map of the study site (Aranser) in relation to nearest three test sites from the International Tree-Ring Databank (ITRDB) that have both RW and MXD data. Inset table details ITRDB code, location, elevation, parameters measured and full period coverage for each site. RW = ring-width, MXD = maximum latewood density and DBI = Delta Blue Intensity. The grey box denotes the regional grid (0-2°E / 42-43°N) of the CRUTS4.02 used for climate analyses. **Lower:** Three example core scans showing the different degrees of colour change.



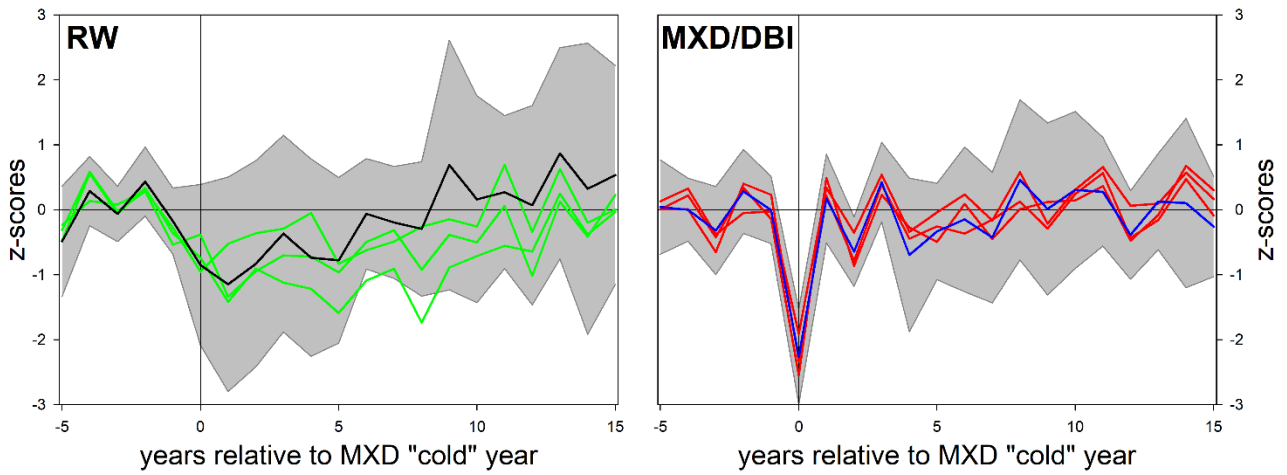
525
526
527
528
529
530
531
532
533
534
535

Figure 2: Comparison of Aranser RW (black) and DBI (blue) chronologies (including correlation matrices - 1783-2004 and mean-interseries correlation values (RBAR)) with appropriate RW (A - green) and MXD (B - red) data from the other three sites. The time-series represent age-dependent spline (with signal free) detrended chronologies transformed to z-scores over the 1783-2004 common period (denoted by vertical dashed line); **C:** Scatter plot of Principal Component Analysis loadings of each chronology on the first two eigenvectors including explained variance on each PC. Legend denotes consistent colour scheme used for all figures; **D:** Mean inter-series correlations (RBAR) of all possible bivariate combinations between the detrended tree series for each site chronology; **E:** Mean 1st-order autocorrelation values for chronology time-series in **A** and **B** calculated over the 1901-2004 period.



536
537
538
539
540
541
542
543

Figure 3: Correlation response function analysis results (1901-2004) between RW (A) and MXD and DBI (B) ADSsf chronologies and monthly and seasonal CRUTS4.02 mean temperature data. **C** and **D** present running 31-year Pearson correlations for RW vs. MJJA and MXD/DBI vs. MJJAS over the same period. 95% confidence limits (CL) are shown for both sets of analyses. The embedded table show correlations between each MXD/DBI chronology with May-September and May-June and August-September seasons for the 1901-1949 and 1950-2004 periods.



544
545
546
547
548
549

Figure 4: Superposed Epoch Analysis for the individual RW and MXD/DBI chronologies for the inferred coldest years (< -2 STDEV below 1883-2004 mean) for all three MXD chronologies (Figure 2B). These years are 1809, 1816, 1829, 1835, 1850, 1910, 1939, 1963 and 1972. The 2-sigma error for the Aranser RW and DBI data are shown with grey shading.